Replication of early and recent Zika virus isolates throughout mouse brain development

Amy B Rosenfeld[1,3]*, David J Doobin[2,3], Audrey L Warren[1], Vincent R Racaniello[1],

Richard B Vallee[2]

[1]Department of Microbiology and Immunology, Columbia University College of

Physicians and Surgeons, New York, New York 10032, USA

[2]Department of Pathology & Cell Biology, Columbia University College of Physicians

and Surgeons, New York, New York 10032, USA

[3]These authors contributed equally to this work

Classification: Biological Sciences, Microbiology

*Correspondence to: Dr. Amy Rosenfeld.

Mailing address: 701 West 168th Street, Hammer Health Science Center 1314,

Columbia University College of Physicians and Surgeons, New York, New York 10032,

USA.

Phone: (212) 305-3796.

Fax: (212) 305-5106.

Email: abr22@cumc.columbia.edu

Abstract

Fetal infection with Zika virus (ZIKV) can lead to congenital Zika virus syndrome (cZVS), which includes cortical malformations and microcephaly. The aspects of cortical development that are affected during virus infection are unknown. Using organotypic brain slice cultures generated from embryonic mice of various ages, sites of ZIKV replication including the neocortical proliferative zone and radial columns, as well as the developing midbrain, were identified. The infected radial units are surrounded by uninfected cells undergoing apoptosis, suggesting that programmed cell death may limit viral dissemination in the brain and may constrain virus associated injury. Therefore, a critical aspect of ZIKV induced neuropathology may be defined by death of uninfected cells. All ZIKV isolates assayed replicated efficiently in early and mid-gestation cultures, and two isolates examined replicated in late-gestation tissue. Alteration of neocortical cytoarchitecture, such as disruption of the highly-elongated basal processes of the radial glial progenitor cells, and impairment of postmitotic neuronal migration were also observed. These data suggest that all lineages of ZIKV tested are neurotropic, and that ZIKV infection interferes with multiple aspects of neurodevelopment that contribute to the complexity of cZVS.

Significance

Zika virus infection has been associated with multiple pathologies of the central nervous system (CNS) including microcephaly, Guillain-Barré syndrome, lissencephaly, the loss of white and grey matter volume and acute myelitis. Using organotypic brain slice cultures, we determined that ZIKV replicates across different embryonic developmental stages, and viral infection can disrupt proper brain development leading to congenital CNS complications. These data illustrate that all lineages of ZIKV tested are neurotropic, and that infection may disrupt neuronal migration during brain development. The results expand our understanding of neuropathologies associated with congenital Zika virus syndrome.

Introduction

Microcephaly is a neurodevelopmental disorder that is clinically characterized by dramatic physical reduction of head circumference (1-3). A variety of etiologies can lead to microcephaly, including vertical transmission of the TORCH microbes: *Toxoplasma gondii*, **R**ubella, **C**ytomegalovirus, **H**erpes simplex virus, or **O**ther pathogens, such as Coxsackievirus, varicella zoster virus, HIV, human T-lymphotropic virus, or *Treponema*. Infection with the arbovirus ZIKV has been associated with the development of congenital cortical malformations including microcephaly (4-15), defining the virus as a new TORCH agent (10, 16).

The reduced head circumference seen with microcephaly is a consequence of reduced brain volume, also manifested in a thinner neocortex. A healthy mature cerebral cortex is composed of six distinct layers of neurons. Most cells within these layers arise from a single layer of apical-basal polarized cells that line the cerebral ventricle (17-23). This single layer of cells undergoes multiple rounds of symmetric mitotic divisions, which largely define the ultimate size of the brain. These cells increasingly undergo asymmetric divisions at which point the cells are referred to as radial glial progenitors (RGPs) (24-26). The asymmetric divisions create two postmitotic daughter cells, with one migrating basally out from the proliferative ventricular zone (VZ) towards the developing cortical plate (CP) of the neocortex. The other cell remains as an RGP attached at the ventricular surface, and the collective progeny of this RGP defines a "radial column." A signature feature of the RGP is its elongated basal fiber that links the VZ to the opposing pial surface. Migration of the postmitotic cells into cortical plate of the developing neocortex occurs along the RGP process (24, 27-31). The late

stages of neocortical development establish the gyri, sulci, and cytoarchitecture of the mature brain. Mutations in genes critical for these processes all may interfere with the proper number of neurons and layers, resulting in a thinner neocortex, consistent with autosomal recessive microcephaly (reviewed in (32)).

Zika virus, a (+) RNA arbovirus in the *Flaviviridae* family, is a re-emerging human pathogen. Originally isolated from a febrile sentinel macaque in 1947, the first reported human infections occurred in Nigeria during the early 1950s (33-36). Initially it was thought that Zika virus infection did not result in clinical disease, but was experimentally neurotropic in mice (33, 36). If symptoms of viral infection were observed in humans, they were mild, including rash, joint pain, and fever (37-43). During the 2007 and 2013 outbreaks in isolated Pacific islands, adult ZIKV infection was associated with neurological dysfunction such as Guillain-Barré syndrome, a disorder in which the immune system attacks the peripheral nervous system, and other central nervous system (CNS) complications (40, 44-54). Once ZIKV spread to the Western Hemisphere, it was recognized to be responsible for the increase of children born with microcephaly and cortical malformations in Brazil and Colombia (9, 55-59). By late 2016, ZIKV infection was known to cause many neurological abnormalities outside of microcephaly, including lissencephaly, loss of brain volume, pachygria, and ventriculomegaly (8, 11, 12, 60-64), which all comprise congenital Zika virus syndrome (cZVS) (4, 5, 8, 11-15).

Several animal models of ZIKV infection including mice and non-human primates have recently been established (65-88). These models illustrate many features of ZIKV induced pathology including viremia and neuronal tissue tropism. The inability to

genetically manipulate non-human primates restricts their use for understanding cZVS. Organoid culture models provide limited information about virus infection of target cells within the context of the developing tissue and organ, since some cell types are missing and there is little to no immune system or vascular representation. Furthermore, many organoid cultures used to understand ZIKV biology only develop neural identity, not tissue organization (89, 90). Organoid cultures do not allow for the study of neuropathologies in the late developing brain, are difficult to consistently manufacture, and are characterized by immature neuronal connectivity; therefore, they are far more simplistic than the brain (91).

Organotypic brain slice cultures are widely used to understand neuronal connectivity and neurodegenerative disorders (92-94), and have enriched our understanding of autosomal-recessive microcephaly and brain development (95, 96). Furthermore, organotypic brain slice cultures from embryonic mice are a genetically amenable system to study cZVS and the ability of the virus to infect neural cells (neurotropism), as the virus inoculum is placed directly on target cells of the cultures. This system fully separates neurotropism from neuroinvasion, virus entry into the CNS from distant sites of the body. Consequently, observations made in organotypic brain slice cultures generated from embryonic mice expand our understanding of viral infection beyond established animal models and organoid cultures.

In this study the effects of ZIKV infection on the embryonic mouse brain were determined using organotypic brain slice cultures. All ZIKV isolates tested from 1947 to the present replicated in early and mid-gestation embryonic brain tissue (E13 and E15, respectively), while two isolates replicated in brain slice cultures from E19 embryos.

Virus replication lead to increased apoptosis within the cultures and impaired neuronal migration into the cortical plate. The results suggest that infection with different isolates of ZIKV can cause severe brain developmental abnormalities. It is likely that brain complexity is reduced through multiple mechanisms during ZIKV infection. These data begin to illuminate how ZIKV-associated neuropathologies develop.

Results

Zika virus neurovirulence is independent of genetic lineage

It has been suggested that neurovirulence was acquired as ZIKV spread from Africa though Asia and Pacific to South America (97). Analysis of the genome sequences of isolates from 1947 to the present defines two phylogenetic groups (Fig. 1). Neurologic disease has been associated with the Asian lineage of viruses (97). To determine if neurotropism is a recently acquired property, replication of virus isolates from both phylogenetic groups was assayed in organotypic brain slice cultures from E15 mouse embryos. Neurogenesis at this stage corresponds to weeks 13/14 in human gestation, the beginning of the second trimester when there is maximal migration of the post-mitotic neurons into the cortical plate (21, 98). Indirect immunofluorescence microscopy (IF) of brain slice cultures 3 days post infection (dpi) with the 2015 Puerto Rican ZIKV isolate revealed virus specific antigen (ZIKV-E) throughout the developing neocortex and midbrain (Fig. 2A). Notably, ZIKV-E was visualized in cells that line the ventricular surface of the developing brain, with staining extending throughout the radial columns of progenitor cells and their neuronal progeny (Fig. 2B). This observation aligns with previous reports that human and mouse neuronal stem cells are a site of ZIKV infection (99, 100). Furthermore, the same phenotype, namely the presence of viral antigen present throughout the cortical plate to the pial surface, was observed in brain slices infected with an isolate acquired from Malaysia during 1996 (Fig. S1).

To determine if E15 brain slice cultures could be productively infected, they were infected with 10^5 pfu of seven ZIKV isolates from 1947 to the present: African [MR766], Senegal, Brazilian, Colombian, Puerto Rican, Honduran and Malaysian (Fig. 2C). At

different times after infection, culture supernatants were harvested and virus production was determined by plaque assay. By 8 dpi, infectious virus was detected in cultures infected with each of the isolates (Fig. 2C). Poliovirus was used as a negative control and did not replicate in brain slice cultures, as the mice used do not produce the poliovirus receptor, CD155 (Fig. 2C).

In previous reports ZIKV infection of human neural progenitor cells produced from induced pluripotent stem cells revealed increased apoptotic cell death (100). Therefore IF analysis was used to detect cleaved caspase 3 in the infected brain slice cultures. There was an increase in apoptosis observed in organotypic slice cultures infected with each ZIKV isolate compared with uninfected cultures (Fig. 3A). Notably, induction of caspase 3 cleavage occurred mostly within the cells that surround the ZIKV infected cell (Fig. 3B), which has also been suggested by the results of other studies (101, 102).

These findings demonstrate that ZIKV infects the embryonic mouse brain during mid-gestation, that the virus is neurotropic independent of its genetic lineage (African or Asian), and that infection leads to apoptosis. The results also establish organotypic embryonic brain slice cultures as a useful system to investigate ZIKV induced brain malformations.

Developmental restraints of Zika virus infection revealed with embryonic organotypic brain slice cultures

The results of epidemiological studies initially suggested that the greatest risks for developing cZVS are associated with maternal ZIKV infection during the first and second trimester (13, 58). Neurological dysfunction has been associated with virus infection during the 3rd trimester, or shortly after birth, albeit less frequently (103-107).

To test whether ZIKV neurotropism is regulated by gestational age, organotypic brain slice cultures were generated from embryonic mice at a range of developmental stages. Brain slices from E13 embryos, which are developmentally comparable to the middle of the first trimester of human neurogenesis, supported viral replication of all 5 ZIKV isolates examined, as determined by expression of a virus specific antigen within focal areas of the neocortex (Fig. 4A, B), and by virus production (Fig. 4C).

Brain slice cultures derived from E19 embryos, which mirror the late stage of neurogenesis during human gestation, supported productive infection with the Honduran and the prototype MR766 isolates (Fig. 5A). During infection with the Honduran isolate, ZIKV E protein was observed only in the neocortex of E19 slices, not within the proliferative zone as seen in E15 infected slices (Fig 5B). These observations mirror those seen during ZIKV infection of late term organoids and in postnatal mice (95, 99, 108). Other ZIKV isolates, including PRV, did not replicate in E19 brain slice cultures (Fig. 5B).

Effects of ZIKV infection on neocortical layer formation

The spectrum of neuronal malformations associated with clinical cZVS is no longer limited to microcephaly. It includes brain calcifications, lissencephaly, ventriculomegaly, cerebellar hypoplasia, and brainstem dysfunction, leading to clinical symptoms including seizures and spasticity (4, 5, 8, 11-15). The wide spectrum of neuropathology seen in patients with cZVS suggests that multiple aspects of brain development may be affected, including neuronal migration. To gain insight as to whether ZIKV replication may alter this behavior, GFP-encoding DNA was electroporated *ex utero* into the radial glial progenitor cells (109) that line the ventricular surface of E15 brains prior to

generation of the organotypic cultures, and infected with ZIKV 24 hr later. IF of organotypic cultures from these brains revealed that ZIKV infection impeded neuronal redistribution as judged by a lower percentage of electroporated cells reaching the most superficial layers of the neocortex 4 dpi (Fig. 6B, C). All of the ZIKV isolates tested impaired neuronal colonization into the cortical plate (Fig. 6A-C).

Microscopic analysis of the infected organotypic slices also revealed that ZIKV infection perturbs the basal projections of the radial glial progenitor cells, marked by vimentin staining (Fig. 6D). Intact radial glial fibers (Fig. 6D, Mock panel) are necessary for proper neuronal migration into the cortical plate. These data support the hypothesis that ZIKV infection can cause structural changes to the basal process of the radial glial progenitor cells and, thereby, impair neuronal migration. A similar scaffold disorganization was observed in ZIKV infected organotypic human fetal brain slices (110) and is an important contributor to other brain developmental diseases (111). Impaired colonization of the cortex with postmitotic neurons is a known cause of autosomal recessive microcephaly and other genetic neurodevelopmental disorders (32). Reduced cortical density may be one mechanism by which congenital Zika virus syndrome develops.

Discussion

Congenital ZIKV syndrome is a significant public health challenge. Microcephalic children may be born to both symptomatic or asymptomatic infected mothers, complicating proper diagnosis and treatment. ZIKV associated neuronal dysfunction may develop postnatally, and there remains a lack of understanding of the long time cognitive and physical disabilities associated with fetal ZKV syndrome (105, 107, 112-117). Many models of ZIKV infection have been established but none have or can systematically examine the consequences of viral infection across pre- and postnatal brain development (65-88, 102, 110, 118).

Mouse brain slices as a model system

The results reported here demonstrate that organotypic brain slice cultures are ideal for studying ZIKV neurotropism. Infection of mouse embryonic brain slice cultures with ZIKV lead to identification of the sites of infection, and visualization of both cell death and impaired neuronal migration into the cortical plate. Although production of organotypic brain slices severs some axonal connections, these cultures nevertheless maintain many aspects of *in vivo* brain biology, including functional local synaptic circuitry with preserved brain architecture, vascularization, and immune composition, and can remain viable for at least 8 days in culture. They can be generated from the exact stage of embryonic development desired. Organoid cultures are unable to faithfully mimic the cellular and structural complexity of the brain, including the presence of a cortical plate, and are heterogeneous with respect to cell type composition and structure, which influences the reproducibility of any findings (91).

Was ZIKV always neurotropic?

Two hypotheses have been suggested to explain the recent epidemic emergence of ZIKV and previously unrecognized neurotropism and congenital disease (97). One possibility is that mutations in the viral genome were selected that enhance transmission and expand tropism of the virus. Alternatively, the virus might have been randomly introduced into large immunologically naïve populations, and the increased numbers of cases revealed previously undetected syndromes. All ZIKV isolates examined, from 1947 to the present, replicated in early and mid-gestation embryonic brain slice cultures (E13 and E15, respectively), demonstrating that ZIKV neurotropism is not a newly acquired characteristic. This observation suggests that the earliest human ZIKV infections could have led to neuronal pathology that was too rare for a clear association to be established, especially in areas with poor health infrastructure. Our findings do not rule out the possibility that mutations within the ZIKV genome have been selected that enhance viral neuroinvasion.

Cell type and developmental stage specificity

The greatest risks for developing cZVS are associated with ZIKV infection during the first and second trimester (13, 58). Our results show that two ZIKV isolates can replicate in brain slice cultures generated from E19 embryos, equivalent to the third trimester of human gestation, yet not all ZIKV isolates replicated in E19 brain slice cultures. For example, the PRV isolate, which replicated in E13 and E15 brain slice cultures, did not replicate in E19 cultures. This observation suggests that the changing cellular environment during embryonic development influences viral neurotropism. Fewer than ten amino acids distinguish PRV from MR766 and the Honduran isolate, but which is the genetic determinant of replication in E19 brain slice cultures will require

further study. Recently it was shown that the PRV isolate replicated in the brain of 1 day old mice inoculated subcutaneously (119). The discrepancy with our results is unexplained, but could involve the genetic background of the mouse or the virus.

Additional brain developmental deficits associated with cZVS have been identified since the first reports of the association of ZIKV infection with microcephaly. These observations are consistent with our understanding that a decrease in neuron number due to either inhibition of RGP proliferation or apoptosis reduces brain size. When apoptosis predominates, areas of programmed cell death contribute not only to an overall microcephalic phenotype, but facilitate the development of neocortical defects such as intracerebral calcifications. Additionally, the neuronal migration defects observed in areas of ZIKV-envelope staining are more typical of the neuropathology associated with lissencephaly. Together these data suggest that multiple mechanisms may contribute to the neuropathology in children diagnosed with cZVS.

Materials and Methods

Ethics Statement. All experiments were performed in accordance with guidelines from the Guide for the Care and Use of Laboratory Animals of the NIH. Protocols were reviewed and approved by the Institutional Animal Care and Use Committee (IACUC) at Columbia University School of Medicine (assurance number AC-AAAR5408).

Cell and organotypic brain slice cultures from embryonic mice and viruses. Vero cells were grown in Dulbecco's modified Eagle medium (Invitrogen, Carlsbad, CA), 10% fetal calf serum (HyClone, Logan, UT), and 1% penicillin-streptomycin (Invitrogen).

Timed pregnant Swiss Webster mice (E13, E15 and E19) were purchased from Taconic Labs; E1 was defined as the day of confirmation of sperm-positive vaginal plug. Mice were sacrificed and fetuses were harvested. Fetal brains were dissected into ice-cold artificial cerebrospinal fluid (ACSF) consisting of 125mM NaCl, 5mM KCl, 1.25mM NaH_2PO_4, 1mM $MgSO_4$, 2mM $CaCl_2$, 25mM $NaHCO_3$, and 20mM glucose, pH7.4, 310 mOsm1^{-1}. Brains were embedded in 4% low melting point agarose dissolved in ACSF and sliced into 300μm coronal sections using a vibratome (Zeiss). Slices were maintained on 0.4 μm, 30mm diameter Millicell-CM inserts (Millipore) in cortical culture medium (CCM) containing 25% Hanks balanced salt solution, 47% basal MEM, 25% normal horse serum, 1X penicillin-streptomycin-glutamine, and 30% glucose. Cultures were maintained in a humidified incubator at 37°C with constant 5% CO_2 supply. Zika viruses (ZIKV) MR766 (Ugandan origin), DAK (Senegal), FLR (Colombia), PRVABC59 (Puerto Rico) and R103451 (Honduras) were obtained from BEI Resources. Brazilian isolate (ZIKV-Paraiba/2015) was kindly provided by Lucia Gama (Johns Hopkins School of Medicine, Baltimore Maryland). All viruses were propagated and assayed in Vero

cells. Viral titers were determined by plaque assay.

***Ex-utero* electroporation.** Plasmids encoding GFP were transfected by intraventricular injection into the ventricle of dissected embryonic brains at the appropriate time. DNA was mixed with colored non-toxic dye and 1μg of nucleic acid was injected into the ventricular space using a high gauge needle made from glass capillary tube. Post injection, five pulses of electrical current (50V, 5ms each, with 1s intervals) were applied by directly placing electrodes on the outer surface of the brain, angled along the lateral aspect of the neocortex adjacent to the lateral ventricle targeted by injection. Brain slices were generated following transfection and cultures were maintained up to 8 days post electroporation.

Indirect immunofluorescence microscopy. Either 72 h, 96h or 8 days post infection, the medium was removed from Zika virus infected or uninfected organotypic brain slices cultures and the cultures were placed overnight in 4% paraformaldehyde (PFA) fixative dissolved in 1X PBS at 4 °C. Following fixation, cultures were incubated in blocking solution of PBS, 0.3% Triton X-100 and 3% donkey serum. Cultures were incubated overnight in at 4 °C in blocking solution containing appropriate primary antibodies. Sections were washed in 1X PBS, and incubated in the presence of fluorophore-conjugated secondary in blocking solution. Sections were mounted on slides using Aqua-Poly/Mount (Polysciences, Inc) and imaged using a iZ80 laser scanning confocal microscope (Olympus FV100 spectral confocal system).

Plaque assay. Vero cells were seeded on 60mm plates for approximately 70% confluence at the time of plaque assay. Next, 100λ portions of serial 10-fold virus dilutions were incubated with cells for 1 h at 37 °C. Two overlays were added to the

infected cells. The first overlay consisted of 2 ml of 1 DMEM, 0.8% Noble agar, 0.1% bovine serum albumin, 40 mM $MgCl_2$, and 10% bovine calf serum. After solidification, a second liquid overlay was added that was composed of 1 DMEM, 0.1% bovine serum albumin, 40 mM $MgCl_2$, 0.2% glucose, 2 mM pyruvate, 4 mM glutamine, and 4 mM oxaloacetic acid. The cells were incubated at 37 °C for 6-8 days and developed by using 10% trichloroacetic acid and crystal violet.

Virus infections. Organotypic brain slice cultures were infected with 10^5 pfu of ZIKV isolates: MR766 African, DHK Senegal, Brazilian, FLR, PRVABC59, and R103451 Honduras, or poliovirus (P1/Mahoney). Virus was allowed to adsorb to the slices for 1h at 37 °C. The inoculum was removed, and the slices were washed 2X in 1X PBS. Infected slices were cultured in CCM for 8 days. 500µl of culture medium was removed and replenished at the described points post infection.

Antibodies. Antibodies used in this study were chicken polyclonal against vimentin (Millipore, AB5733, 1:1000 dilution), pan-flavivirus E glycoprotein (Millipore, MAB 10216), rabbit polyclonal against CDP (Santa-Cruz, SC-1302), and cleaved caspase 3 (Cell Signaling) Donkey fluorophore-conjugated secondary antibodies (Jackson Labs, 1:500 dilution) were used together with DAPI (4',6-diamidino-2-phenylindole, Thermo Scientific, 62248, 1:1,000 dilution).

Data Analysis. GraphPad Prism software was used to analyze all data. Log10-transformed titers were used for graphing the results of plaque assays.

Acknowledgments

References

1. Barkovich AJ*, et al.* (1996) A classification scheme for malformations of cortical development. *Neuropediatrics* 27(2):59-63.
2. Mochida GH (2009) Genetics and biology of microcephaly and lissencephaly. *Semin Pediatr Neurol* 16(3):120-126.
3. Mochida GH & Walsh CA (2001) Molecular genetics of human microcephaly. *Curr Opin Neurol* 14(2):151-156.
4. Driggers RW*, et al.* (2016) Zika Virus Infection with Prolonged Maternal Viremia and Fetal Brain Abnormalities. *N Engl J Med* 374(22):2142-2151.
5. Moura da Silva AA*, et al.* (2016) Early Growth and Neurologic Outcomes of Infants with Probable Congenital Zika Virus Syndrome. *Emerg Infect Dis* 22(11):1953-1956.
6. Gatherer D & Kohl A (2016) Zika virus: a previously slow pandemic spreads rapidly through the Americas. *J Gen Virol* 97(2):269-273.
7. Martines RB*, et al.* (2016) Notes from the Field: Evidence of Zika Virus Infection in Brain and Placental Tissues from Two Congenitally Infected Newborns and Two Fetal Losses--Brazil, 2015. *MMWR Morb Mortal Wkly Rep* 65(6):159-160.
8. Mlakar J*, et al.* (2016) Zika Virus Associated with Microcephaly. *N Engl J Med* 374(10):951-958.
9. Schuler-Faccini L*, et al.* (2016) Possible Association Between Zika Virus Infection and Microcephaly - Brazil, 2015. *MMWR Morb Mortal Wkly Rep* 65(3):59-62.
10. Franca GV*, et al.* (2016) Congenital Zika virus syndrome in Brazil: a case series of the first 1501 livebirths with complete investigation. *Lancet* 388(10047):891-897.
11. Besnard M*, et al.* (2016) Congenital cerebral malformations and dysfunction in fetuses and newborns following the 2013 to 2014 Zika virus epidemic in French Polynesia. *Euro Surveill* 21(13).
12. Miranda-Filho Dde B*, et al.* (2016) Initial Description of the Presumed Congenital Zika Syndrome. *Am J Public Health* 106(4):598-600.
13. Brasil P*, et al.* (2016) Zika Virus Infection in Pregnant Women in Rio de Janeiro - Preliminary Report. *N Engl J Med*.
14. Cauchemez S*, et al.* (2016) Association between Zika virus and microcephaly in French Polynesia, 2013-15: a retrospective study. *Lancet* 387(10033):2125-2132.
15. Strafela P*, et al.* (2016) Zika Virus-Associated Micrencephaly: A Thorough Description of Neuropathologic Findings in the Fetal Central Nervous System. *Arch Pathol Lab Med*.
16. Steele RW (2016) Zika Virus: An Explosive Pandemic and a New TORCH Agent. *Clin Pediatr (Phila)* 55(8):698-700.
17. Spemann H (1938) *Embryonic Development and Induction* (Yale University Press, New Haven, Connecticut).
18. Bentivoglio M & Mazzarello P (1999) The history of radial glia. *Brain Res Bull* 49(5):305-315.
19. Rakic P (2003) Elusive radial glial cells: historical and evolutionary perspective. *Glia* 43(1):19-32.

20. Ramon y Cajal S (1991) *Histologie de Systeme Nerveus de l'Homme et des Vertebres.* (Consejo Superior de Investigaciones, Maloine, Paris).
21. Sidman RL & Rakic P (1973) Neuronal migration, with special reference to developing human brain: a review. *Brain Res* 62(1):1-35.
22. Noctor SC*, et al.* (2002) Dividing precursor cells of the embryonic cortical ventricular zone have morphological and molecular characteristics of radial glia. *J Neurosci* 22(8):3161-3173.
23. Noctor SC, Flint AC, Weissman TA, Dammerman RS, & Kriegstein AR (2001) Neurons derived from radial glial cells establish radial units in neocortex. *Nature* 409(6821):714-720.
24. Rakic P (1971) Guidance of neurons migrating to the fetal monkey neocortex. *Brain Res* 33(2):471-476.
25. Rakic P (1972) Mode of cell migration to the superficial layers of fetal monkey neocortex. *J Comp Neurol* 145(1):61-83.
26. Schmechel DE & Rakic P (1979) A Golgi study of radial glial cells in developing monkey telencephalon: morphogenesis and transformation into astrocytes. *Anat Embryol (Berl)* 156(2):115-152.
27. Vignal W (1888) Arch Physiol Norm Pathol. 2:338.
28. Ramon y Cajal S (1893) *Cellule* 7:125.
29. Kolliker A (1896) *Handbuch der Gewebelehre des Menchen* (Leipzig).
30. Stefanowka M (1898) *Trav lab Invest* 2:1.
31. Rakic P (1974) Neurons in rhesus monkey visual cortex: systematic relation between time of origin and eventual disposition. *Science* 183(4123):425-427.
32. Faheem M*, et al.* (2015) Molecular genetics of human primary microcephaly: an overview. *BMC Med Genomics* 8 Suppl 1:S4.
33. Dick GW (1952) Zika virus. II. Pathogenicity and physical properties. *Trans R Soc Trop Med Hyg* 46(5):521-534.
34. Dick GW, Kitchen SF, & Haddow AJ (1952) Zika virus. I. Isolations and serological specificity. *Trans R Soc Trop Med Hyg* 46(5):509-520.
35. Macnamara FN (1952) Annual Report, Virus Research Institute, Nigeria, for 1951-52.
36. Macnamara FN (1954) Zika virus: a report on three cases of human infection during an epidemic of jaundice in Nigeria. *Trans R Soc Trop Med Hyg* 48(2):139-145.
37. Simpson DI (1964) Zika Virus Infection in Man. *Trans R Soc Trop Med Hyg* 58:335-338.
38. Bearcroft WG (1956) Zika virus infection experimentally induced in a human volunteer. *Trans R Soc Trop Med Hyg* 50(5):442-448.
39. CDC (2016) Zika Virus. (Center for Disease Control and Prevention, Atlanta, GA).
40. Duffy MR*, et al.* (2009) Zika virus outbreak on Yap Island, Federated States of Micronesia. *N Engl J Med* 360(24):2536-2543.
41. Musso D*, et al.* (2014) Potential for Zika virus transmission through blood transfusion demonstrated during an outbreak in French Polynesia, November 2013 to February 2014. *Euro Surveill* 19(14).

42. Cerbino-Neto J*, et al.* (2016) Clinical Manifestations of Zika Virus Infection, Rio de Janeiro, Brazil, 2015. *Emerg Infect Dis* 22(7):1318-1320.

43. Lazear HM & Diamond MS (2016) Zika Virus: New Clinical Syndromes and Its Emergence in the Western Hemisphere. *J Virol* 90(10):4864-4875.

44. Pinto-Diaz CA*, et al.* (2017) Autoimmunity in Guillain-Barre syndrome associated with Zika virus infection and beyond. *Autoimmun Rev*.

45. Cao-Lormeau VM*, et al.* (2016) Guillain-Barre Syndrome outbreak associated with Zika virus infection in French Polynesia: a case-control study. *Lancet* 387(10027):1531-1539.

46. Musso D, Nilles EJ, & Cao-Lormeau VM (2014) Rapid spread of emerging Zika virus in the Pacific area. *Clin Microbiol Infect* 20(10):O595-596.

47. Oehler E*, et al.* (2014) Zika virus infection complicated by Guillain-Barre syndrome--case report, French Polynesia, December 2013. *Euro Surveill* 19(9).

48. ECDC (2014)in *Rapid Risk Assessment: Zika Virus Infection Outbreak, French Polynesia.* (European Centre for Disease Prevention and Control, Stockholm, Sweden).

49. Roze B*, et al.* (2016) Zika virus detection in cerebrospinal fluid from two patients with encephalopathy, Martinique, February 2016. *Euro Surveill* 21(16).

50. Roze B*, et al.* (2016) Zika virus detection in urine from patients with Guillain-Barre syndrome on Martinique, January 2016. *Euro Surveill* 21(9):30154.

51. Thomas DL*, et al.* (2016) Local Transmission of Zika Virus--Puerto Rico, November 23, 2015-January 28, 2016. *MMWR Morb Mortal Wkly Rep* 65(6):154-158.

52. Broutet N*, et al.* (2016) Zika Virus as a Cause of Neurologic Disorders. *N Engl J Med* 374(16):1506-1509.

53. Carteaux G*, et al.* (2016) Zika Virus Associated with Meningoencephalitis. *N Engl J Med* 374(16):1595-1596.

54. Sejvar JJ, Baughman AL, Wise M, & Morgan OW (2011) Population incidence of Guillain-Barre syndrome: a systematic review and meta-analysis. *Neuroepidemiology* 36(2):123-133.

55. Kleber de Oliveira W*, et al.* (2016) Increase in Reported Prevalence of Microcephaly in Infants Born to Women Living in Areas with Confirmed Zika Virus Transmission During the First Trimester of Pregnancy - Brazil, 2015. *MMWR Morb Mortal Wkly Rep* 65(9):242-247.

56. Cavalheiro S*, et al.* (2016) Microcephaly and Zika virus: neonatal neuroradiological aspects. *Childs Nerv Syst* 32(6):1057-1060.

57. Campos GS, Bandeira AC, & Sardi SI (2015) Zika Virus Outbreak, Bahia, Brazil. *Emerg Infect Dis* 21(10):1885-1886.

58. Pacheco O*, et al.* (2016) Zika Virus Disease in Colombia - Preliminary Report. *N Engl J Med*.

59. Faria NR*, et al.* (2016) Zika virus in the Americas: Early epidemiological and genetic findings. *Science* 352(6283):345-349.

60. Zare Mehrjardi M*, et al.* (2017) Neuroimaging findings of congenital Zika virus infection: a pictorial essay. *Jpn J Radiol* 35(3):89-94.

61.   de Fatima Vasco Aragao M, *et al.* (2016) Clinical features and neuroimaging (CT and MRI) findings in presumed Zika virus related congenital infection and microcephaly: retrospective case series study. *BMJ* 353:i1901.

62.   Hazin AN, *et al.* (2016) Computed Tomographic Findings in Microcephaly Associated with Zika Virus. *N Engl J Med* 374(22):2193-2195.

63.   Ventura CV, Maia M, Bravo-Filho V, Gois AL, & Belfort R, Jr. (2016) Zika virus in Brazil and macular atrophy in a child with microcephaly. *Lancet* 387(10015):228.

64.   Centers for Disease C (

65.   Lazear HM, *et al.* (2016) A Mouse Model of Zika Virus Pathogenesis. *Cell Host Microbe* 19(5):720-730.

66.   Rossi SL, *et al.* (2016) Characterization of a Novel Murine Model to Study Zika Virus. *Am J Trop Med Hyg* 94(6):1362-1369.

67.   Miner JJ, *et al.* (2016) Zika Virus Infection during Pregnancy in Mice Causes Placental Damage and Fetal Demise. *Cell* 165(5):1081-1091.

68.   Miner JJ, *et al.* (2016) Zika Virus Infection in Mice Causes Panuveitis with Shedding of Virus in Tears. *Cell Rep* 16(12):3208-3218.

69.   Li C, *et al.* (2016) Zika Virus Disrupts Neural Progenitor Development and Leads to Microcephaly in Mice. *Cell Stem Cell* 19(1):120-126.

70.   Li H, *et al.* (2016) Zika Virus Infects Neural Progenitors in the Adult Mouse Brain and Alters Proliferation. *Cell Stem Cell*.

71.   Cugola FR, *et al.* (2016) The Brazilian Zika virus strain causes birth defects in experimental models. *Nature* 534(7606):267-271.

72.   van den Pol AN, Mao G, Yang Y, Ornaghi S, & Davis JN (2017) Zika Virus Targeting in the Developing Brain. *J Neurosci* 37(8):2161-2175.

73.   Vermillion MS, *et al.* (2017) Intrauterine Zika virus infection of pregnant immunocompetent mice models transplacental transmission and adverse perinatal outcomes. *Nat Commun* 8:14575.

74.   Tripathi S, *et al.* (2017) A novel Zika virus mouse model reveals strain specific differences in virus pathogenesis and host inflammatory immune responses. *PLoS Pathog* 13(3):e1006258.

75.   Smith DR, *et al.* (2017) Neuropathogenesis of Zika Virus in a Highly Susceptible Immunocompetent Mouse Model after Antibody Blockade of Type I Interferon. *PLoS Negl Trop Dis* 11(1):e0005296.

76.   Aliota MT, *et al.* (2016) Heterologous Protection against Asian Zika Virus Challenge in Rhesus Macaques. *PLoS Negl Trop Dis* 10(12):e0005168.

77.   Coffey LL, *et al.* (2017) Zika Virus Tissue and Blood Compartmentalization in Acute Infection of Rhesus Macaques. *PLoS One* 12(1):e0171148.

78.   Duggal NK, *et al.* (2017) Frequent Zika Virus Sexual Transmission and Prolonged Viral RNA Shedding in an Immunodeficient Mouse Model. *Cell Rep* 18(7):1751-1760.

79.   Fernandes NC, *et al.* (2017) Experimental Zika virus infection induces spinal cord injury and encephalitis in newborn Swiss mice. *Exp Toxicol Pathol* 69(2):63-71.

80.   Hirsch AJ, *et al.* (2017) Zika Virus infection of rhesus macaques leads to viral persistence in multiple tissues. *PLoS Pathog* 13(3):e1006219.

81.   Koide F, *et al.* (2016) Development of a Zika Virus Infection Model in Cynomolgus Macaques. *Front Microbiol* 7:2028.

82. Li XF, *et al.* (2016) Characterization of a 2016 Clinical Isolate of Zika Virus in Non-human Primates. *EBioMedicine* 12:170-177.
83. Osuna CE, *et al.* (2016) Zika viral dynamics and shedding in rhesus and cynomolgus macaques. *Nat Med* 22(12):1448-1455.
84. Pardi N, *et al.* (2017) Zika virus protection by a single low-dose nucleoside-modified mRNA vaccination. *Nature* 543(7644):248-251.
85. Singh PK, *et al.* (2017) Zika virus infects cells lining the blood-retinal barrier and causes chorioretinal atrophy in mouse eyes. *JCI Insight* 2(4):e92340.
86. Xavier-Neto J, *et al.* (2017) Hydrocephalus and arthrogryposis in an immunocompetent mouse model of ZIKA teratogeny: A developmental study. *PLoS Negl Trop Dis* 11(2):e0005363.
87. Li C, *et al.* (2017) 25-Hydroxycholesterol protecs host against Zika virus infection and its associated microcephaly in a mouse model. *Immunity* 46:1-11.
88. Adams Waldorf KM, *et al.* (2016) Fetal brain lesions after subcutaneous inoculation of Zika virus in a pregnant nonhuman primate. *Nat Med* 22(11):1256-1259.
89. Lancaster MA, *et al.* (2013) Cerebral organoids model human brain development and microcephaly. *Nature* 501(7467):373-379.
90. Gabriel E, *et al.* (2017) Recent Zika Virus Isolates Induce Premature Differentiation of Neural Progenitors in Human Brain Organoids. *Cell Stem Cell* 20(3):397-406 e395.
91. Qian X, Nguyen HN, Jacob F, Song H, & Ming GL (2017) Using brain organoids to understand Zika virus-induced microcephaly. *Development* 144(6):952-957.
92. Gahwiler BH & Hefti F (1984) Guidance of acetylcholinesterase-containing fibres by target tissue in co-cultured brain slices. *Neuroscience* 13(3):681-689.
93. Gahwiler BH, Capogna M, Debanne D, McKinney RA, & Thompson SM (1997) Organotypic slice cultures: a technique has come of age. *Trends Neurosci* 20(10):471-477.
94. Cho S, Wood A, & Bowlby MR (2007) Brain slices as models for neurodegenerative disease and screening platforms to identify novel therapeutics. *Curr Neuropharmacol* 5(1):19-33.
95. Doobin DJ, Kemal S, Dantas TJ, & Vallee RB (2016) Severe NDE1-mediated microcephaly results from neural progenitor cell cycle arrests at multiple specific stages. *Nat Commun* 7:12551.
96. Baffet AD, *et al.* (2016) Cellular and subcellular imaging of motor protein-based behavior in embryonic rat brain. *Methods Cell Biol* 131:349-363.
97. Weaver SC (2017) Emergence of Epidemic Zika Virus Transmission and Congenital Zika Syndrome: Are Recently Evolved Traits to Blame? *MBio* 8(1).
98. Rakic P, Cameron RS, & Komuro H (1994) Recognition, adhesion, transmembrane signaling and cell motility in guided neuronal migration. *Curr Opin Neurobiol* 4(1):63-69.
99. Qian X, *et al.* (2016) Brain-Region-Specific Organoids Using Mini-bioreactors for Modeling ZIKV Exposure. *Cell* 165(5):1238-1254.
100. Tang H, *et al.* (2016) Zika Virus Infects Human Cortical Neural Progenitors and Attenuates Their Growth. *Cell Stem Cell* 18(5):587-590.

101. Simonin Y, *et al.* (2016) Zika Virus Strains Potentially Display Different Infectious Profiles in Human Neural Cells. *EBioMedicine* 12:161-169.
102. Brault JB, *et al.* (2016) Comparative Analysis Between Flaviviruses Reveals Specific Neural Stem Cell Tropism for Zika Virus in the Mouse Developing Neocortex. *EBioMedicine* 10:71-76.
103. Soares de Souza A, *et al.* (2016) Fetal Infection by Zika Virus in the Third Trimester: Report of 2 Cases. *Clin Infect Dis*.
104. Nunes AT, *et al.* (2016) Comparative proteome analysis reveals that blood and sugar meals induce differential protein expression in Aedes aegypti female heads. *Proteomics* 16(19):2582-2586.
105. Soares de Oliveira-Szejnfeld P, *et al.* (2016) Congenital Brain Abnormalities and Zika Virus: What the Radiologist Can Expect to See Prenatally and Postnatally. *Radiology* 281(1):203-218.
106. Melo AS, *et al.* (2016) Congenital Zika Virus Infection: Beyond Neonatal Microcephaly. *JAMA Neurol*.
107. van der Linden V, *et al.* (2016) Description of 13 Infants Born During October 2015-January 2016 With Congenital Zika Virus Infection Without Microcephaly at Birth - Brazil. *MMWR Morb Mortal Wkly Rep* 65(47):1343-1348.
108. Huang WC, Abraham R, Shim BS, Choe H, & Page DT (2016) Zika virus infection during the period of maximal brain growth causes microcephaly and corticospinal neuron apoptosis in wild type mice. *Sci Rep* 6:34793.
109. Imayoshi I, *et al.* (2013) Oscillatory control of factors determining multipotency and fate in mouse neural progenitors. *Science* 342(6163):1203-1208.
110. Onorati M, *et al.* (2016) Zika Virus Disrupts Phospho-TBK1 Localization and Mitosis in Human Neuroepithelial Stem Cells and Radial Glia. *Cell Rep* 16(10):2576-2592.
111. Carabalona A, *et al.* (2012) A glial origin for periventricular nodular heterotopia caused by impaired expression of Filamin-A. *Hum Mol Genet* 21(5):1004-1017.
112. McCarthy M (2016) Zika congenital syndrome is seen in infants whose mothers had asymptomatic infection. *BMJ* 353:i3416.
113. McCarthy M (2016) Zika related microcephaly may appear after birth, study finds. *BMJ* 355:i6333.
114. Moore CA, *et al.* (2017) Characterizing the Pattern of Anomalies in Congenital Zika Syndrome for Pediatric Clinicians. *JAMA Pediatr* 171(3):288-295.
115. Panchaud A, Stojanov M, Ammerdorffer A, Vouga M, & Baud D (2016) Emerging Role of Zika Virus in Adverse Fetal and Neonatal Outcomes. *Clin Microbiol Rev* 29(3):659-694.
116. Kapogiannis BG, Chakhtoura N, Hazra R, & Spong CY (2017) Bridging Knowledge Gaps to Understand How Zika Virus Exposure and Infection Affect Child Development. *JAMA Pediatr*.
117. Prevention CfDCa (2017) Congenital Zika Virus Infection Initial Evaluation.
118. Retallack H, *et al.* (2016) Zika virus cell tropism in the developing human brain and inhibition by azithromycin. *Proc Natl Acad Sci U S A*.
119. Manangeeswaran M, Ireland DD, & Verthelyi D (2016) Zika (PRVABC59) Infection Is Associated with T cell Infiltration and Neurodegeneration in CNS of Immunocompetent Neonatal C57Bl/6 Mice. *PLoS Pathog* 12(11):e1006004.

Figure Legends

Figure 1. Phylogenetic tree of ZIKV isolates used in this work. Entire genome sequences of 7 ZIKV isolates examined in this study were aligned using the ClustalW module of DNAstar.

Figure 2. Representative tissue distribution and replication of ZIKV isolates in organotypic mouse brain slices. (A) Brain slice cultures from E15 embryos were infected with 10^5 pfu of the ZIKV PRV isolate, and at 4 dpi were fixed and stained with pan-flavivirus antibody against the E glycoprotein (ZIKV-E) and DAPI. Scale bar is 500 μm. **(B)** Higher magnification (60x objective) of the ventricular surface of infected brain slice culture, stained with pan-flavivirus antibody. Scale bar is 10 μm. **(C)** Time course of replication of multiple isolates of ZIKV in E15 brain slice cultures.

Figure 3. ZIKV infection of organotypic mouse brain slices leads to increased apoptosis. (A) Brain slice cultures from E15 embryos were infected with 10^5 pfu of the indicated ZIKV isolates or poliovirus, and at 8 dpi were fixed and stained with pan-flavivirus antibody against the E glycoprotein (ZIKV-E), antibody to cleaved caspase 3 (CC3), and DAPI. Scale bar is 100 μm. **(B)** Higher magnification (60x objective) of PRV ZIKV infected slices from panel A. Scale bar is 10 μm. **(C)** Apoptotic index, as defined by number of cleaved CC3 positive cells per square micron, in E15 brain slice cultures infected with the indicated ZIKV isolates. PV, poliovirus.

Figure 4. ZIKV replicates in early gestation neural tissue. (A, B) Brain slice cultures from E13 embryos were infected with 10^5 pfu of the indicated ZIKV isolates, and at 8 dpi were fixed and stained with pan-flavivirus antibody against the E glycoprotein (ZIKV-E) and DAPI. Scale bar is 250 μm. **(C)** Time course of replication of multiple isolates of ZIKV in E13 brain slice cultures.

Figure 5. Replication of two ZIKV isolates in late gestation neural tissue. (A, B) Brain slice cultures from E19 embryos were infected with 10^5 pfu of the indicated ZIKV isolates, and at 8 dpi were fixed and stained with pan-flavivirus antibody against the E glycoprotein (Z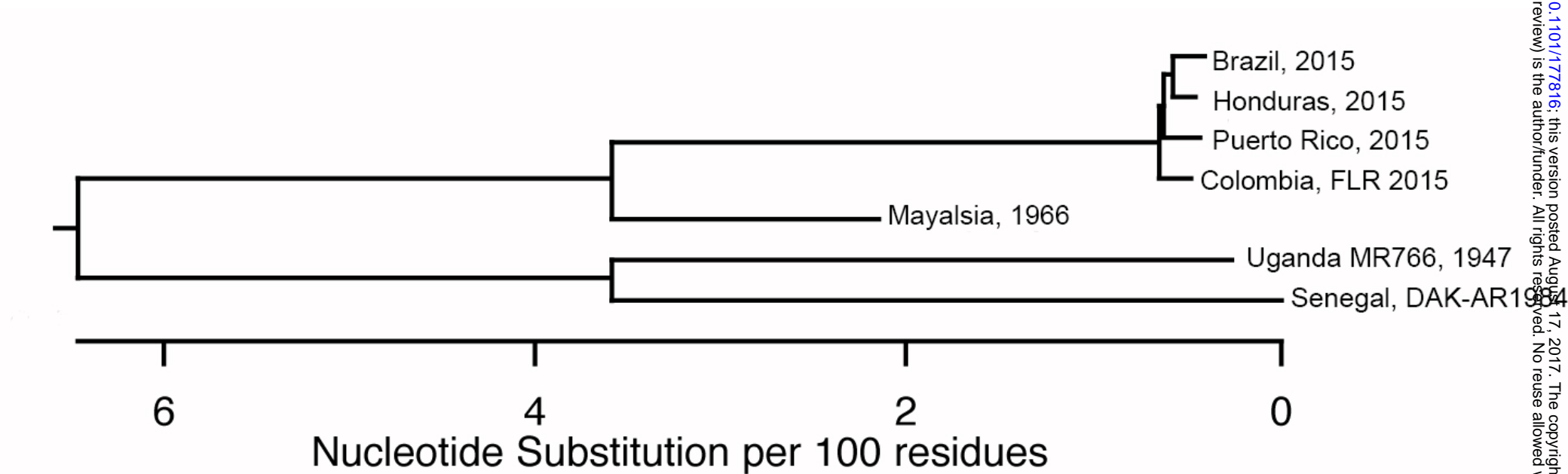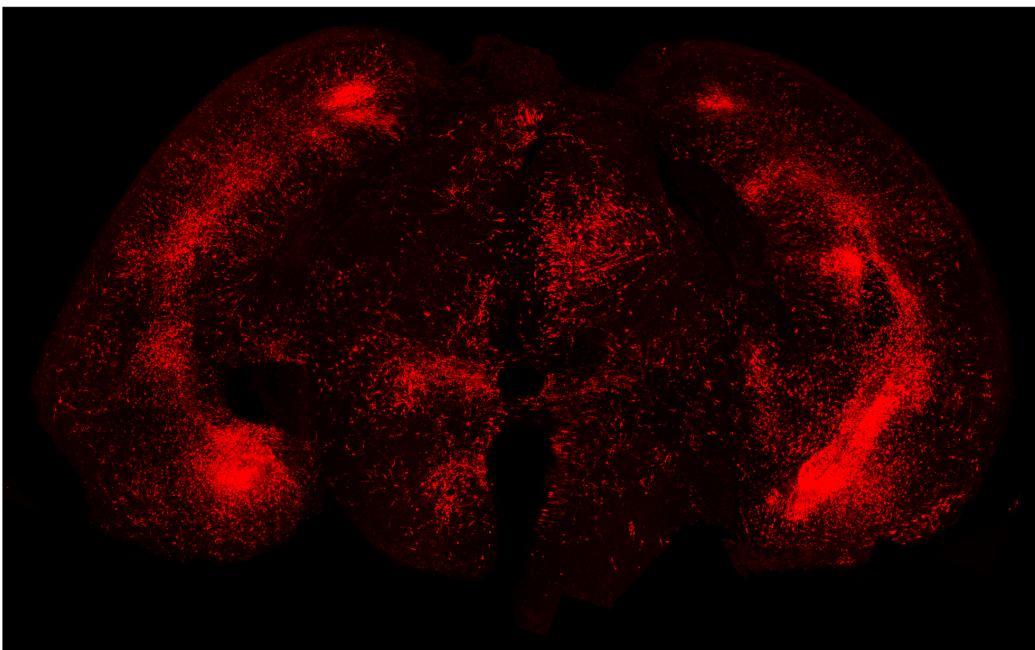IKV-E), cleaved caspase 3 (CC3) and DAPI. Scale bar is 500 and 250 μm in **(A)** and **(B)**. **(C)** Time course of replication of multiple isolates of ZIKV in E19 brain slice cultures. P1/Mahoney, DHK, Colombian, and PRV isolates did not replicate are the lines are superimposed and not readily visible.

Figure 6. Neuronal migration is impaired during ZIKV infection. (A) Plasmid encoding GFP DNA was electroporated into E19 brains ex utero prior to production of slice cultures. Twenty-four hours later, the slice cultures were infected with 10^5 pfu of the indicated ZIKV isolates, and at 4 dpi were fixed and stained with pan-flavivirus antibody against the E glycoprotein (ZIKV-E), antibody against cortical layer 2-4 marker Tbr1, and DAPI. **(B)** The cortical plate was divided into six regions of equal size, and the percentage of GFP fluorescent intensity in each sector over the whole six sectors was calculated. **(C)** Distribution of GFP positive cells within each sector for mock and ZIKV infected slices. 1 is the pial surface, and 6 is the ventricular surface. Data represented

as mean ± SEM for each condition in each bin in **(C)**. Unpaired t-test was used to determine significance (* for p<0.05, n=3 embryonic brains across different replicate experiments). **(D)** Sections from panel **(A)** were stained with antibody against the E glycoprotein (ZIKV-E), and antibody against vimentin to mark the radial glia progenitor (RGP) basal processes, which are the tracks upon which bipolar neurons migrate, and with DAPI. Scale bar is 250 μm for **(A)** and **(D)**.

Supplemental Figure 1. **Tissue distribution and replication of Malaysian ZIKV isolate in E15 organotypic mouse brain slices.** Brain slice cultures from E15 embryos were infected with 10^5 pfu of the Malaysian ZIKV isolate, and at 4 dpi were fixed and stained with pan-flavivirus antibody against the E glycoprotein (ZIKV-E), cleaved caspase 3 (CC3) and DAPI. Scale bar is 500 μm.

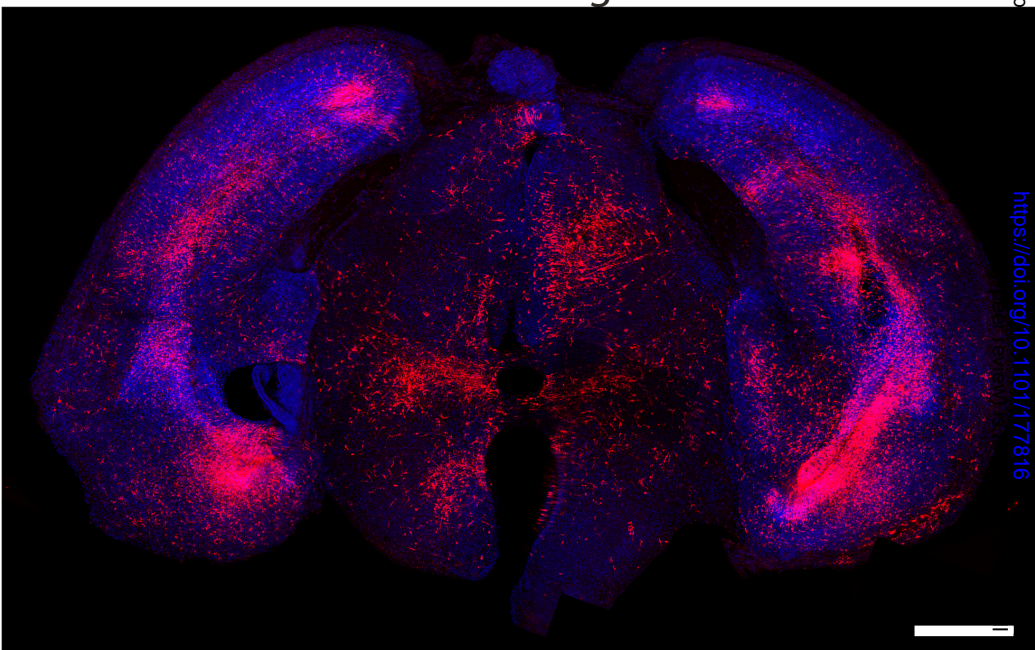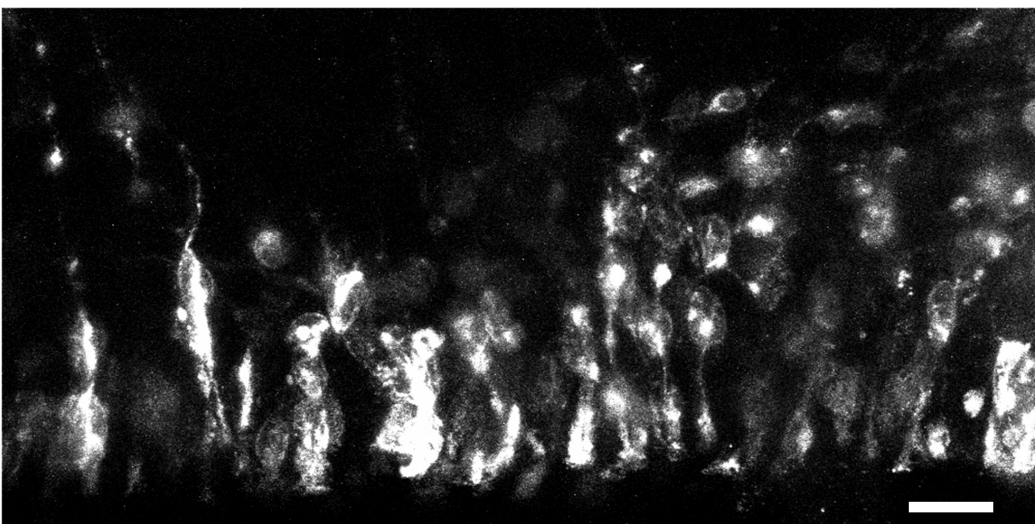Brazil, 2015
Honduras, 2015
Puerto Rico, 2015
Colombia, FLR 2015
Mayalsia, 1966
Uganda MR766, 1947
Senegal, DAK-AR1984

Nucleotide Substitution per 100 residues

6   4   2   0

Figure 1

A ZIKV-E | DAPI/Merge

B ZIKV-E

C

Legend for panel C:
- PV (poliovirus)
- MR 766 (Uganda, 1947)
- DHK (Senegal, 1984)
- Brazil (Brazil, 2015)
- PRV (Puerto Rico, 2015)
- Colombian (Colombia, 2015)
- Honduran (Honduras, 2016)
- Malaysian (Malaysia, 1966)

Y-axis: PFU/ml
1×10^{8}, 1×10^{7}, 1×10^{6}, 1×10^{5}, 1×10^{4}, 1×10^{3}, 1×10^{2}, 1×10^{1}, 1×10^{0}, 1×10^{-1}

X-axis: Days Post Infection
0, 2, 4, 6, 8, 10
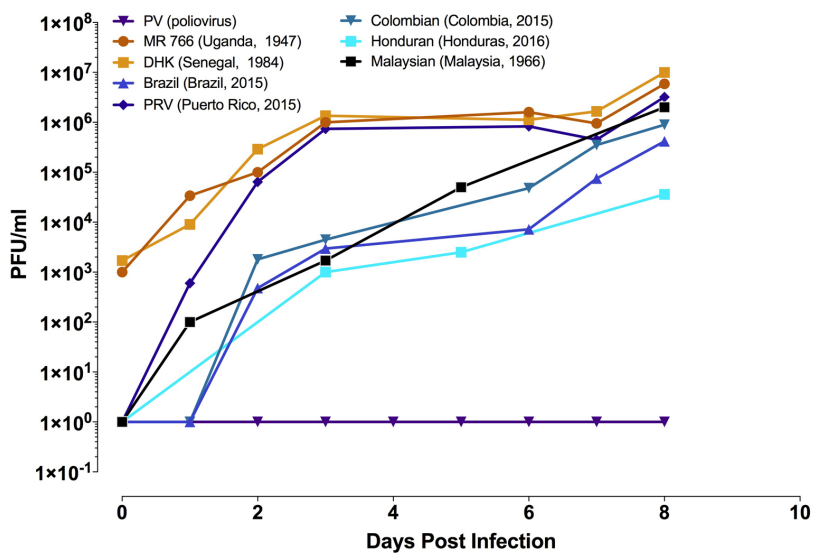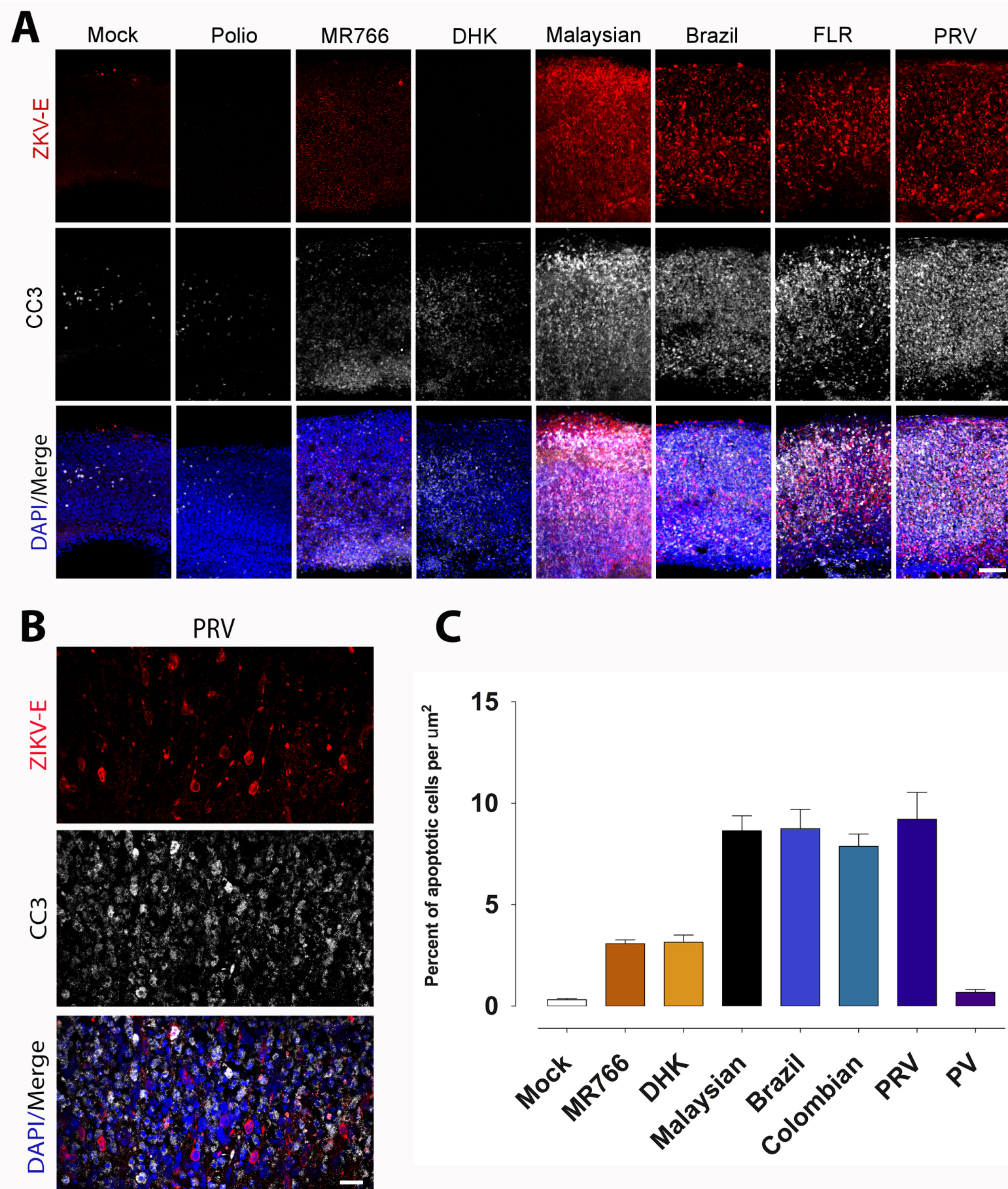
Figure 2

Figure 3

Figure 4

Figure 5

A

Mock   DHK   Brazil   FLR

ZIKV-E

pUB-GFP

Tbr1

Merge

B

C

Percent of GFP Signal in each cortical plate layer

- Mock
- DHK
- Brazil
- FLR

Cortical Plate Layer Bin

D

Mock   DHK   PRV

ZIKV-E

Vimentin

DAPI/ Merge

Figure 6

Malaysian

ZIKV-E

CC3

DAPI/Merge

Figure S1